Int J Adv Manuf Technol (2008) 35:814–820
DOI 10.1007/s00170-006-0758-1

ORIGINAL ARTICLE

Effects of punch load for elliptical deep drawing product of automotive parts

Dong Hwan Park · Prasad K. D. V. Yarlagadda

Received: 4 February 2005 / Accepted: 8 August 2005 / Published online: 14 November 2006

Abstract Deep drawing process, one of sheet metal forming methods, is very useful in industrial field because of its efficiency. The production of optimal products using this process is dependent on the process variables such as blank shapes, profile radii of punch and die, and formability of materials. Of the variables, the blank shape is very important since it controls the formability factor. This paper reports the investigations on three kinds of blank shapes and the scribed circle test on three deformation modes. The punch load distribution for elliptical forming processes were measured under different conditions of profile radii of punch and die and discussed here. These experiments clarified the influence of the profile radii of the punch and die and the blank shape on the punch-load distribution for the elliptical deep drawing product of automobile parts. The aim of this study is to investigate the effect that the process variables have on drawability in a non-axisymmetric elliptical deep-drawing process and to obtain useful data from the industrial field.

Keywords Deep-drawing process · Blank shape · Punch load · Profile radii · Punch stroke · Process variables

1 Introduction

The sheet-metal forming processes have an important role in industries such as automobile, airplane, and electric appliance due to their advantages in reducing development time and final cost of the products. In general, sheet-metal forming may involve stretching, drawing, repetition of bending and unbending or various combinations of these basic modes of deformation. Many studies on the process variables of cylindrical products have been carried out regarding the fundamentals of deep drawing process. Thus, many shapes such as rectangular, elliptical and non-axisymmetrical have been produced. In general, most of the research for deep-drawing process has addressed the formability of axisymmetrical shapes, but there have been few studies done on the formability of elliptical shapes. Sheet metal can deform only to a certain level before a localized zone of thinning or necking occurs. This level is dependent mainly on the combination of the ratio of major and minor strains. Keeler (1965) first introduced the forming limit diagram (FLD). Keeler's work was limited to conditions of biaxial stretching, i.e. when both major and minor principal surface strains were positive. Goodwin (1968) extended Keeler's work to include the tension-compression principal strain region. This combined diagram is now well known as the Keeler-Goodwin forming limit diagram [1]. The FLD is widely used in industry as a guide on the formability of sheet metal deformation processes.

In order to obtain the optimum elliptical deep-drawing product with a non-axisymmetric shape, many process variables such as material property, profile radii of punch and die, lubrication condition, ram speed, blank holding force (BHF), clearance, and so on must be considered before the drawability of the product can be determined. Besides, profile radii of punch and die and blank shape are the most important variables that influence the formability in deep drawing process [2–4]. The formability of the deep-drawing process can be promoted, and lead time and cost can be reduced by choosing both appropriate profile radii of a punch and die and blank shape for the deep-drawing process [5–6].

D. H. Park (✉) · P. K. D. V. Yarlagadda
School of Mechanical, Manufacturing and Medical Engineering,
Queensland University of Technology,
Gardens Point Campus, 2 George Street, P.O. Box 2434,
Brisbane Qld 4001, Australia
e-mail: pdhwan@pusan.ac.kr

The formability of non-axisymmetric shapes has been explored under the press conditions that the blank size is different between the major and minor axes and that the material flow is non-uniform. It is important to change the blank shape, because a blank comes into contact with the die. As the area of contact increases between the blank holder and the die, the blank holding force and the punch force increase. This is a reason for forming defects by increased deformation resistance. To solve this defect, many studies into the shape of blanks have been performed in circular and rectangular deep drawing, but there have not been sufficient studies concerning the shape of blanks in elliptical deep drawing [7–22]. In this study, the profile radii of punch and die and blank shapes influence on formability in the elliptical deep drawing process has been investigated by analyzing the punch load distribution.

2 Deep-drawing experiment

2.1 Experimental material

The material used was SECD (KS: Korean standards) with high quality formability and a thickness of 1.6 mm. This was galvanized with 20 μm of zinc. Tensile tests were carried out in the directions of 0, 45, and 90° to the rolling direction. The gauge length and width of the tensile specimens were 25 and 50 mm, respectively. The mechanical property in the tensile direction is indicated in Table 1. The specimens for the tensile tests were cut by a wire-electric spark machine and based on the KS B 0801 No. 5. The tensile strength of the specimens was measured through the tensile test using UTM with setting load speed as 10 mm/min.

2.2 Experimental equipment and conditions

Figure 1 shows the applied equipment, hydraulic press (100 tons) with a die-cushion to control the blank holding force and limit the switch to determine a stroke of upper ram according to the processes. Also the equipment has a computer which has a linear variable differential transformer (LVDT). When the steel sheet is formed in this equipment, the LVDT measures the punch load according to punch stroke.

Table 1 Mechanical property in the tensile direction

Direction	Young's module (Gpa)	Yield strength (Mpa)	Tensile strength (Mpa)	Elongation (%)
0°	50.9	182	426	48.4
45°	54.5	200	433	41.4
90°	58.5	205	412	48.2
Average	54.6	195.7	423.7	46

Fig. 1 Experimental equipment for elliptical deep drawing

Table 2 shows the experimental conditions for profile radii of the punch and die. The punch profile radius (R_p) was fixed at 6.4 mm, the die profile radius (R_d) was selected based on two conditions. The punch stroke for the experiment consists of three strokes which are (1) 46 mm in the first process; (2) 62 mm in the second process; and (3) 74 mm in the third process. The blank holding pressure was applied to 2 N/mm^2. The lubricant for the operation of deep drawing used was a soluble oil lubrication for plastic working. Figure 2 presents the die geometry of the non-axisymmetric elliptical deep drawing process used in this test.

2.3 Scribed circle test

The plane deformation resulting from the formation of a sheet metal workpiece can be measured by using an array of small diameter (10 mm) circles, printed on the blank surface in the critical strain regions. Figure 3 shows scribed circle marks of a non-axisymmetric blank. The circles deform into various shapes during forming, the major and minor axes indicate the direction of the major and minor principal strains. Likewise, the measured dimensions are used to determine the major and minor principal strain magnitudes. This circular grid technique of measuring strains can be used to diagnose the causes of necking and fracture in industrial practice and to investigate whether these defects were caused by variations in the properties of the material, wear of the tools, changes in lubrication, or incorrect press settings.

Table 2 The experimental conditions for punch and die Profile radii

	First process R_{d1} (mm)	Second process R_{d2} (mm)	Third process R_{d3} (mm)	Remark (mm)
Blank type (A, B, C)	11.2	11.2	11.2 16	R_p=6.4
		16	11.2 16	
	16	11.2	11.2 16	
		16	11.2 16	

In non-axisymmetric elliptical deep drawing, three modes of forming regimes are found: draw, stretch, and plane strain. The draw mode for non-axisymmetric elliptical deep drawing could be defined when the major and minor strains are positive. The stretch mode could be defined when the major strain is positive and minor strain is negative, and plane strain mode could be defined when the major strain is positive and minor strain is zero. Figures 4, 5, and 6 present the major and minor strain distribution by scribed circle test after the first drawing according to the punch and die radii. From the result of the scribed circle test, the three deformation modes of the major and minor strains for non-axisymmetric elliptical deep drawing are shown in Fig. 7. The wall and flange of deformation zones are mainly applied to the draw mode, the punch head is applied to the plane strain mode, and the corner is applied to the stretch mode.

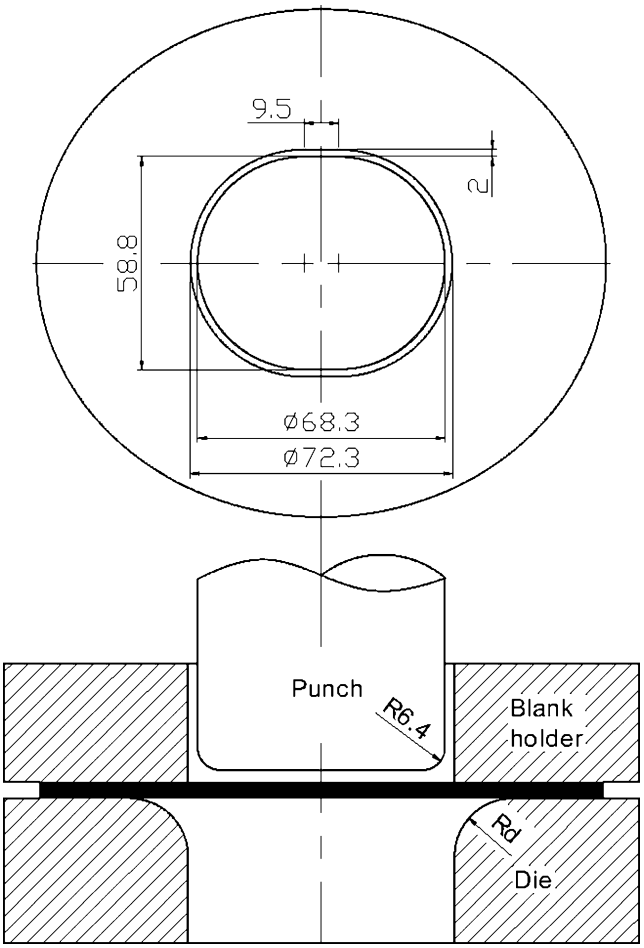

Fig. 2 Die geometry of elliptical deep drawing

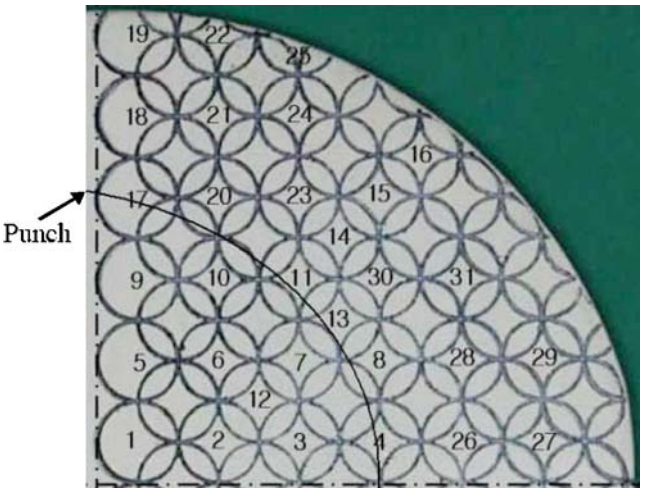

Fig. 3 Scribed circle marks of non-axisymmetric blank

3 Blank shape design

Generally, the trial-and-error method based on the experiences of skilled toolmakers, which increases the amount of time and costs, has been tried for developing the blank shape. Therefore, in this study, in order to design the blank shape which is equivalent to the surface area of the final product,

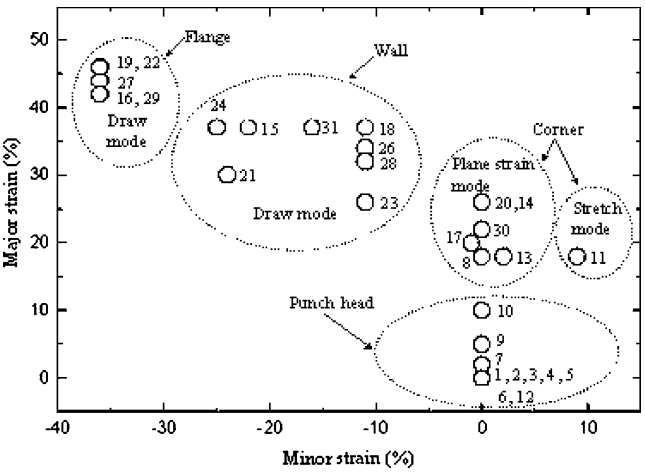

Fig. 4 Major and minor strain distribution after the first drawing (R_p= 6.4 mm, R_d=6.4 mm)

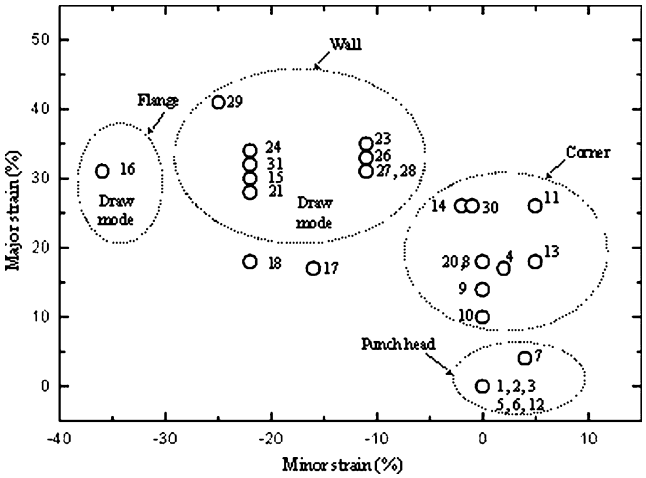

Fig. 5 Major and minor strain distribution after the first drawing (R_p= 6.4 mm, R_d=11.2 mm)

we calculated the surface area of the final product by means of three-dimensional modeling [4–6]. We used three kinds of blanks, which have an equivalent surface area to the final product. Figure 8 shows the geometry of shapes. The outline of the type A blank is larger than the type B and C blanks. The short side length of the type B blank is smaller than the type C blank. On the other hand, the long side length of the type B blank is a little larger than the type C blank. The process of the applied product in the experiment consists of seven stages of the deep drawing process and three stages of trimming, restriking etc. So, the total number of multi-deep drawing stages is 10. In this study, the experiment to measure punch load was performed from the first process to the third process. Figure 9 shows the product shape of each type blank according to process.

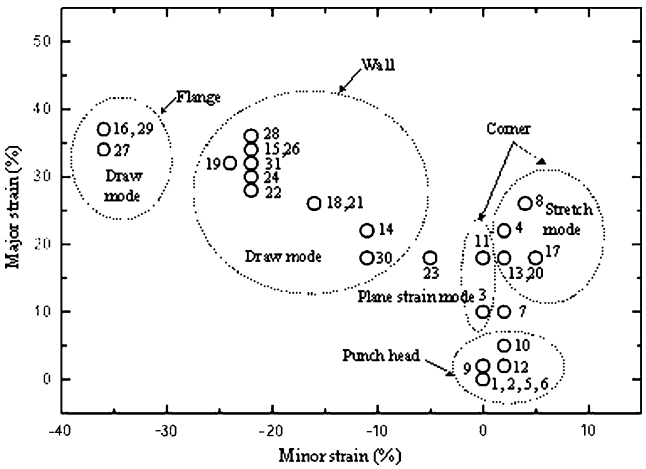

Fig. 6 Major and minor strain distribution after the first drawing (R_p= 6.4 mm, R_d=16 mm)

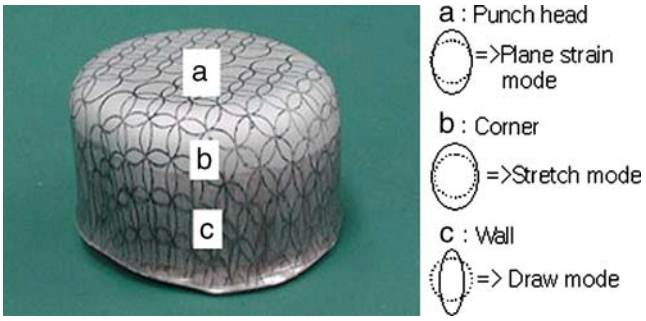

Fig. 7 Three deformation modes of major and minor strains

4 Result and discussions

Figure 10 shows the comparison of the punch load along the blank types in the first process. The punch profile radius (R_p) was fixed at 6.4 mm, the die profile radius (R_{d1}) of the first process was selected under two conditions, 11.2 and 16 mm. As a non-axisymmetric blank draws in the die cavity, the initial punch load increased rapidly causing inflow resistance of the long and short sides and then the maximum punch load is measured as 55% of the punch stroke. After the maximum punch load, the load was reduced and then forming was completed until the bottom dead center (BDC) of the punch stroke. Work hardening of the steel sheet occurred due to the increase of the amount of deformation as the punch arrives at the BDC of punch stroke. The punch stroke is finished at top dead center (TDC).

The punch load of the type A blank measured relatively large in comparison with the type B and C blanks, and the punch loads of the type B and C blanks were similar. The area of the type A blank is on the whole large in comparison with the type B and C blanks. In other words,

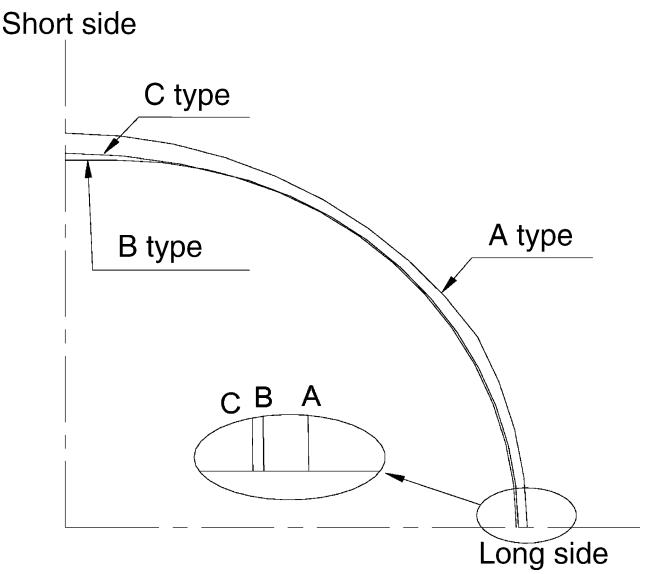

Fig. 8 Geometry of blank shapes

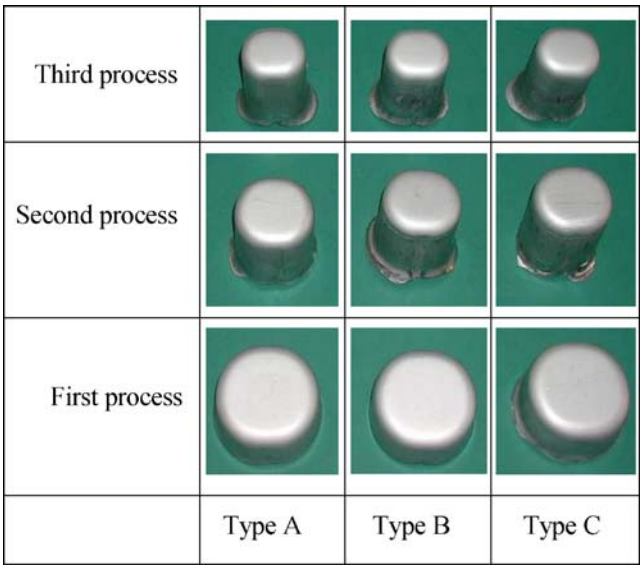

Fig. 9 Product shapes of each type blank

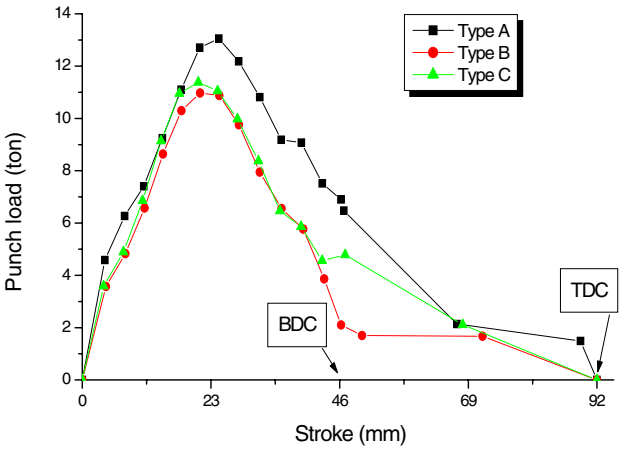

(a) Punch load-stroke curve of each blank type (R_{d1}=11.2)

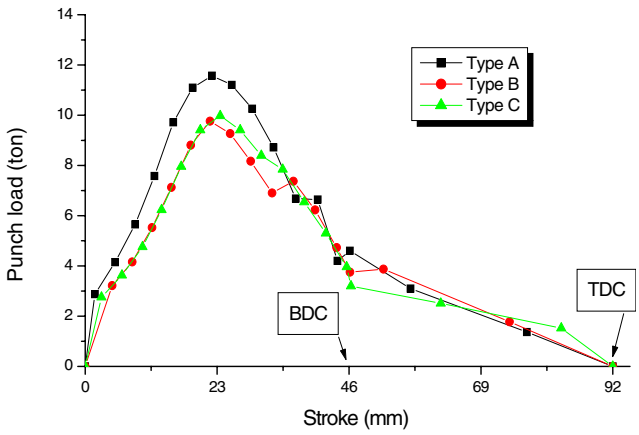

(b) Punch load-stroke curve of each blank type (R_{d1}=16)

Fig. 10 Comparison of the punch load along the blank types in the first drawing (R_p=6.4 mm)

the contact surface area of the blank holder of the type A blank is larger than that of the type B and C blanks. Therefore, it is considered that the largest value of the punch load is measured at the type A blank where the high blank holding force is needed due to the large contact surface area of the blank holder. Table 3 shows the maximum punch load of the blank shapes along the die profile radii in the first process. The maximum punch load when R_{d1}=16 mm is smaller than when it is R_{d1}=11.2 mm.

Figure 11 shows the comparison of the punch load along the blank types in the second process. The punch profile radius (R_p) was fixed at 6.4 mm, the die profile radius (R_{d1}) of the first process was fixed at 16 mm, and the die profile radius (R_{d2}) of the second process was selected under two conditions, 11.2 and 16 mm. The maximum punch load was measured at 80% of the punch stroke when the type A, B blanks were used, and was measured at 60% of the punch stroke when the type C blank was used as shown in Fig. 6. As we compared with the punch load along each process, the punch load of the second process was smaller than the first process and the results of experiments showed that the punch load of the three types of blanks was similar. The punch load is small while the blank draws from the first to the second process due to the reduced drawing length.

Figure 12 shows the comparison of the punch load along the blank types in the third process. The punch profile radius (R_p) was fixed at 6.4 mm, we compared the two conditions: the one die profile radii (R_d) of the first, second and third process was fixed at 16 mm; the other die profile radii (R_{d1}) of the first, second and third process was fixed at 11.2 mm.

The punch load of the type A blank was relatively large in comparison with the type B and C blanks, while the punch stroke made progress when R_d=11.2 mm as shown in Fig. 12a. Figure 12b shows the similar punch load without a large difference about the three types, after BDC of the punch stroke. We attributed some difference of the punch load to friction between the punch and the steel sheet as shown in Figs. 10, 11 and 12. If the maximum punch load is larger than the fracture force (P_F) to shear the steel sheet when forming a non-axisymmetric elliptical product, then

Table 3 The maximum punch load of blank shapes along the die profile radii in the first process (R_p=6.4) (unit: tons)

Die profile radii	Type A	Type B	Type C
R_{d1}=11.2	13.1	10.9	11.4
R_{d1}=16	11.2	9.8	9.9

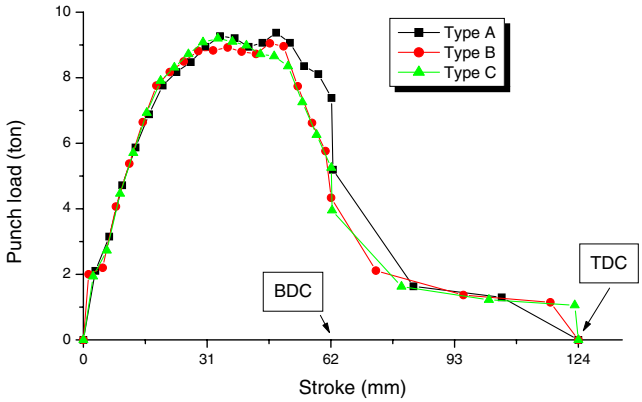

(a) Punch load-stroke curve of each blank type (R_{d1}=16, R_{d2}=11.2)

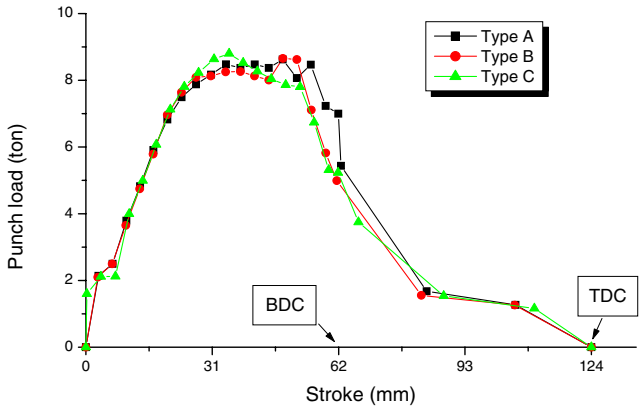

(b) Punch load-stroke curve of each blank type (R_{d1}=16, R_{d2}=16)

Fig. 11 Comparison of the punch load along the blank types in the second drawing (R_p=6.4 mm)

the fracture occurred at that time. Theoretically P_F is calculated as follows.

$$P_F = Lt\sigma_b = 210 \times 1.6 \times 43.29$$

The fracture force (P_F) was calculated using the drawing length (L) of the blanks. It is 14.5 tons. Therefore, the maximum punch load measured in the experiments, 13.1 tons, was performed without the fracture of the non-axisymmetric elliptical product.

Because the type A blank is larger than the type B and C blanks, the blank holding force increased. Therefore, the punch load of the type A blank shows a large value in every process due to an increase of the blank holding force. In contrast to the type A blank, because the punch load of the type B and C blanks is smaller than that of the type A blank, the blank holding force is reduced. Therefore, the punch load of the type B and C blanks shows a small value for every process due to the reduced blank holding force. Although the punch load is similar to that in the type B blank, a good product that has no discontinuous section could make from the type C blank. Therefore, we expect that the type C blank will be applied in the industrial field in the near future.

5 Conclusions

In this study, we carried out experiments on the deep-drawing product with steel sheets for drawability for an elliptical product. Therefore, the conclusion of these experiments clarified the influence of the profile radii of the punch and die and the blank shape on the punch load distribution for non-axisymmetric elliptical deep drawing products. The results are summarized as follows.

1. From the result of scribed circle test, the wall and flange of deformation zones are mainly applied to the draw mode, the punch head is applied to the plane strain mode, and the corner is applied to the stretch mode

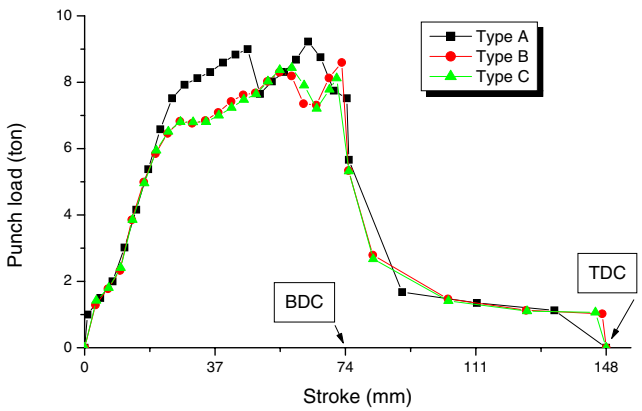

(a) Punch load-stroke curve of each blank type (R_{d1}=11.2, R_{d2}=11.2, R_{d3}=11.2)

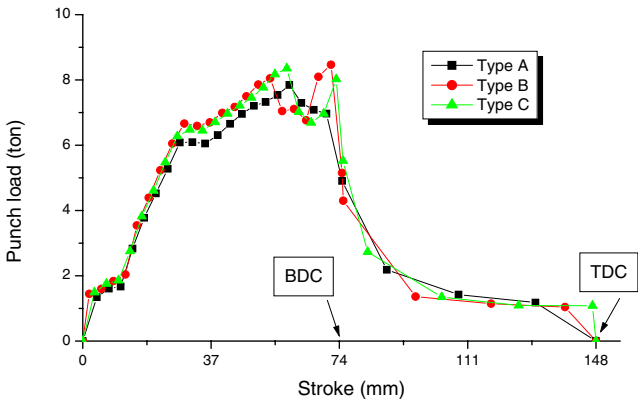

(b) Punch load-stroke curve of each blank type (R_{d1}=16, R_{d2}=16, R_{d2}=16)

Fig. 12 Comparison of the punch load along the blank types in the third process (R_p=6.4 mm)

2. We could see that the maximum punch load was reduced gradually as the process progressed
3. We could see that the maximum punch load of the type A blank had the largest value among the three kinds of blanks during the process and although the type C blank's punch load is similar to that of the type B blank, good products without discontinuous section could be obtained from the type C blank

References

1. McCandless AJ, Bahrani AS (1979) Strain paths, limit strains and forming limit diagram. 7th NAMRC, SME, May 2000, pp 184-190
2. Kim DH (1998) Experimental study on minimizing wall thickness thinning for deep drawing of circular shells. J Korean Soc Tech Plastic 7(4):393–399
3. Majlessi SA, Lee D (1993) Deep drawing square-shape sheet metal parts, part 1: finite element analysis. ASME J Eng Ind 115:102–109
4. Marumo Y, Saiki H (1998) Estimation of the deep drawability of aluminum square cups by fracture forces. Met Mater Int 4(3):372–375
5. Park DH, Bae WR, Park SB, Kang SS (1999) An experimental study on optimization of blank shape in elliptical deep drawing process. J Korean Soc Prec Eng 16(10):101–108
6. Park DH, Bae WR, Park SB, Kang SS (2000) Application surface area calculating system for design of blank shape of deep drawing product. J Korean Soc Prec Eng 17(4):97–105
7. Yasunori Saotome, Kaname Yasuda, Hiroshi Kaga (2001) Micro-deep drawability of very thin sheet steels. J Mater Process Technol 113:641–647
8. Heo YM, Wang SH, Kim HY, Seo DG (2001) The effect of the drawbead dimensions of the weld-line movements in the deep drawing of taylor-welded blanks. J Mater Process Technol 113:686–691
9. Kapinski S (1996) Analytical and experimental analysis of deep drawing process for bimetal elements. J Mater Process Technol 60:197–200
10. Li R, Weinmann KJ (1999) Formability in non-symmetric aluminium panel drawing using active drawbeads. Annal CIRP 48(1):209–212
11. Park SH, Yoon JW, Yang DY, Kim YH (1999) Optimum blank design in sheet metal forming by the deformation path iteration method. Int J Mech Sci 41:1217–1232
12. Lee KS, Huh H (1998) Finite element simulation of three dimensional superplastic blow forming. Metal Mater Int 4(3):299–305
13. Yang DY, Lee SW, Kim JB, Yoon JW, Lee DW (1998) Holistic design and simulation system in sheet metal forming processes. Metal Mater Int 4(4):715–722
14. Cho CS, Lee CH, Huh H (1997) Design of process parameters in axisymmetric multi-step deep drawing by a finite element inverse method. J Korean Soc Tech Plastic 6(4):300–310
15. Yoon JW, Yang DY, Chung K, Barlat F (1999) A general elasto-plastic finite element formulation based on incremental deformation theory for planar anisotropy and its application to sheet metal forming. Int J Mech Sci 15:35–67
16. Chen FK (1997) Analysis of an equivalent drawbead model for the finite element simulation of a stamping process. Int J Mach Tools Manuf 37(4):409–423
17. Hung YM, Li CL (1999) An elasto-plastic finite element analysis of the metal sheet redrawing process. J Mater Process Technol 89:331–338
18. Leu DK (1997) Prediction of the limiting drawing ratio and the maximum drawing load in cup drawing. Int J Mach Tools Manuf 37(2):201–213
19. Leu DK, Chen TC, Huang YM (1999) Influence of punch shapes on the collar-drawing process of sheet steel. J Mater Process Technol 88:134–146
20. Ceretti E, Giardini C, Maccarini G (1995) Theoretical and experimental analysis of non-axisymmetrical deep drawing. J Mater Process Technol 54:375–384
21. Doege E, El-Dsoki T, Seibert D (1995) Prediction of necking and wrinkling in sheet-metal forming. J Mater Process Technol 50:197–206
22. Rao KP, Mohan EVR (2001) A unified test for evaluating material parameters for use in the modeling of sheet metal forming. J Mater Process Technol 113:725–731